

Single walled carbon nanotube growth and chirality dependence on catalyst composition

Alvin W. Orbaek, Andrew C. Owens, Christopher C. Crouse, Cary L. Pint, Robert H. Hauge, and Andrew R. Barron*

Department of Chemistry, Rice University, Houston, TX 77005, USA.

Department of Mechanical Engineering and Materials Science, Rice University, Houston,
TX 77005, USA.

College of Engineering, Swansea University, Singleton Park, Swansea SA2 8PP, Wales,
UK.

Supplementary information

Table S1. Experimental values used for the synthesis of iron oxide and bi-metallic oxide nanoparticles

| Sample | Fe(acac) ₃ (mmol) | M(acac) _x (mmol) | 1,2-HDD (mmol) | Oleic acid (mmol) | Oleyl amine (mmol) | % Fe ICP-AES |
|--------------------------------|---------------------------------|--------------------------------|-------------------|----------------------|-----------------------|-----------------|
| Fe ₃ O ₄ | 0.75 | 0 | 1.5 | 3 | 3 | 100 |
| <i>l</i> -Mn-Fe-O | 0.5 | 0.25 | 1.5 | 3 | 3 | 91 |
| <i>h</i> -Mn-Fe-O | 0.225 | 0.525 | 1.5 | 3 | 3 | 63 |
| <i>l</i> -Co-Fe-O | 0.7125 | 0.0375 | 1.5 | 3 | 3 | 97 |
| <i>h</i> -Co-Fe-O | 0.5 | 0.25 | 1.5 | 3 | 3 | 67 |
| <i>l</i> -Ni-Fe-O | 0.7125 | 0.0375 | 1.5 | 3 | 3 | 94 |
| <i>h</i> -Ni-Fe-O | 0.5 | 0.25 | 1.5 | 3 | 3 | 69 |
| <i>l</i> -Cu-Fe-O | 0.5 | 0.25 | 1.5 | 3 | 3 | 98 |
| <i>h</i> -Cu-Fe-O | 0.45 | 0.3 | 1.5 | 3 | 3 | 76 |

Table S2. Number of independent growth runs for each catalyst composition.

| | <i>l</i> -Mn-Fe | <i>h</i> -Mn-Fe | Fe ₃ O ₄ | <i>l</i> -Co-Fe | <i>h</i> -Co-Fe | <i>l</i> -Ni-Fe | <i>h</i> -Ni hi | <i>l</i> -Cu-Fe | <i>h</i> -Cu-Fe |
|--------|-----------------|-----------------|--------------------------------|-----------------|-----------------|-----------------|-----------------|-----------------|-----------------|
| 514 nm | 8 | 10 | 14 | 9 | 6 | 7 | 8 | 8 | 9 |
| 633 nm | 5 | 6 | 7 | 5 | 6 | 7 | 7 | 7 | 7 |
| 785 nm | 11 | 5 | 3 | 5 | 4 | 3 | 7 | 12 | 4 |

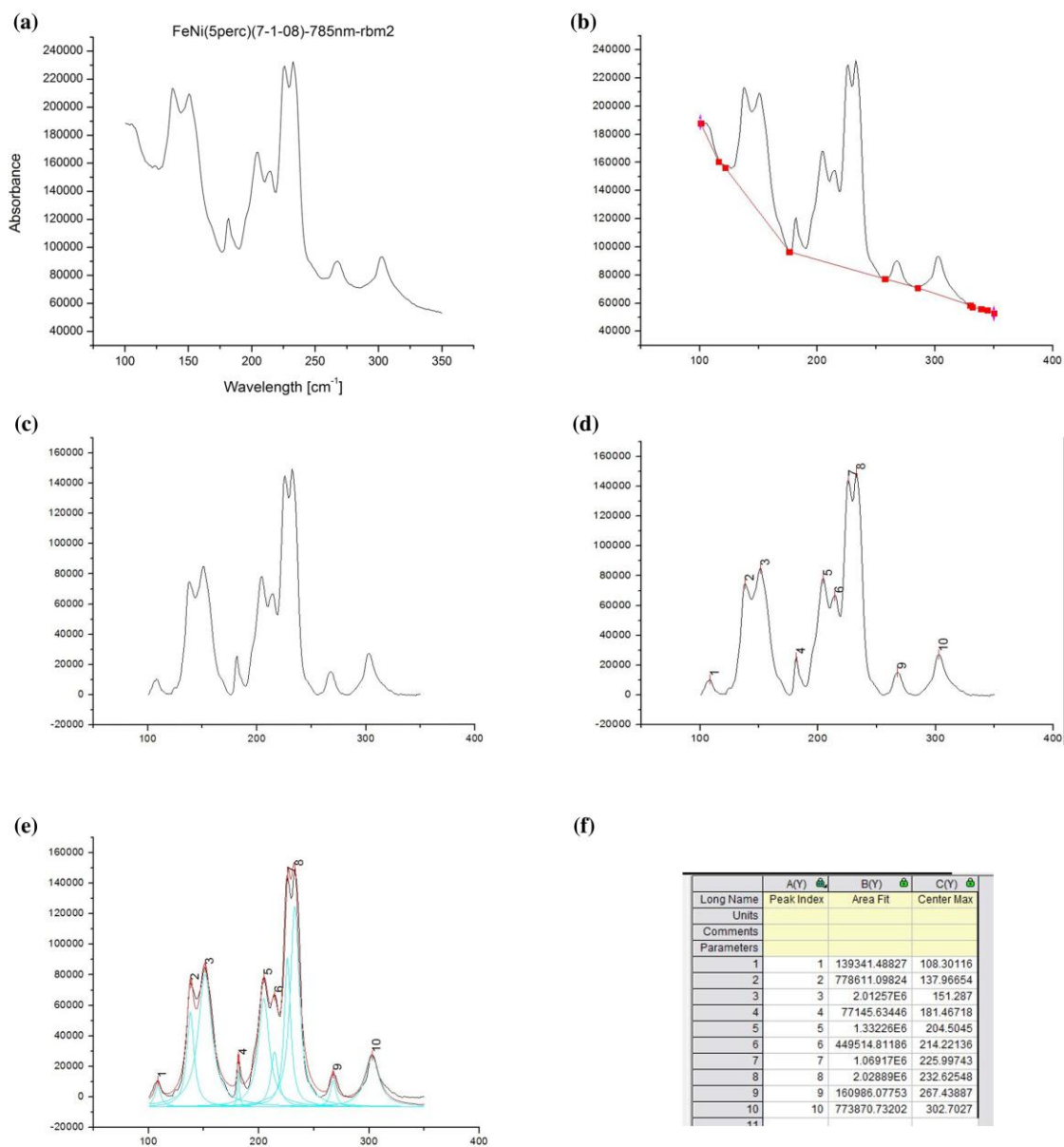


Figure S1. Protocol used to fit Raman data starting with raw data (a) the baseline is first determined (b), and then subtracted (c). The peaks are then identified (d) and the area under the peaks obtained (e). The data is exported for further use (f) such that the peaks for each set of raw data is determined and the respective volume under each peak determined.

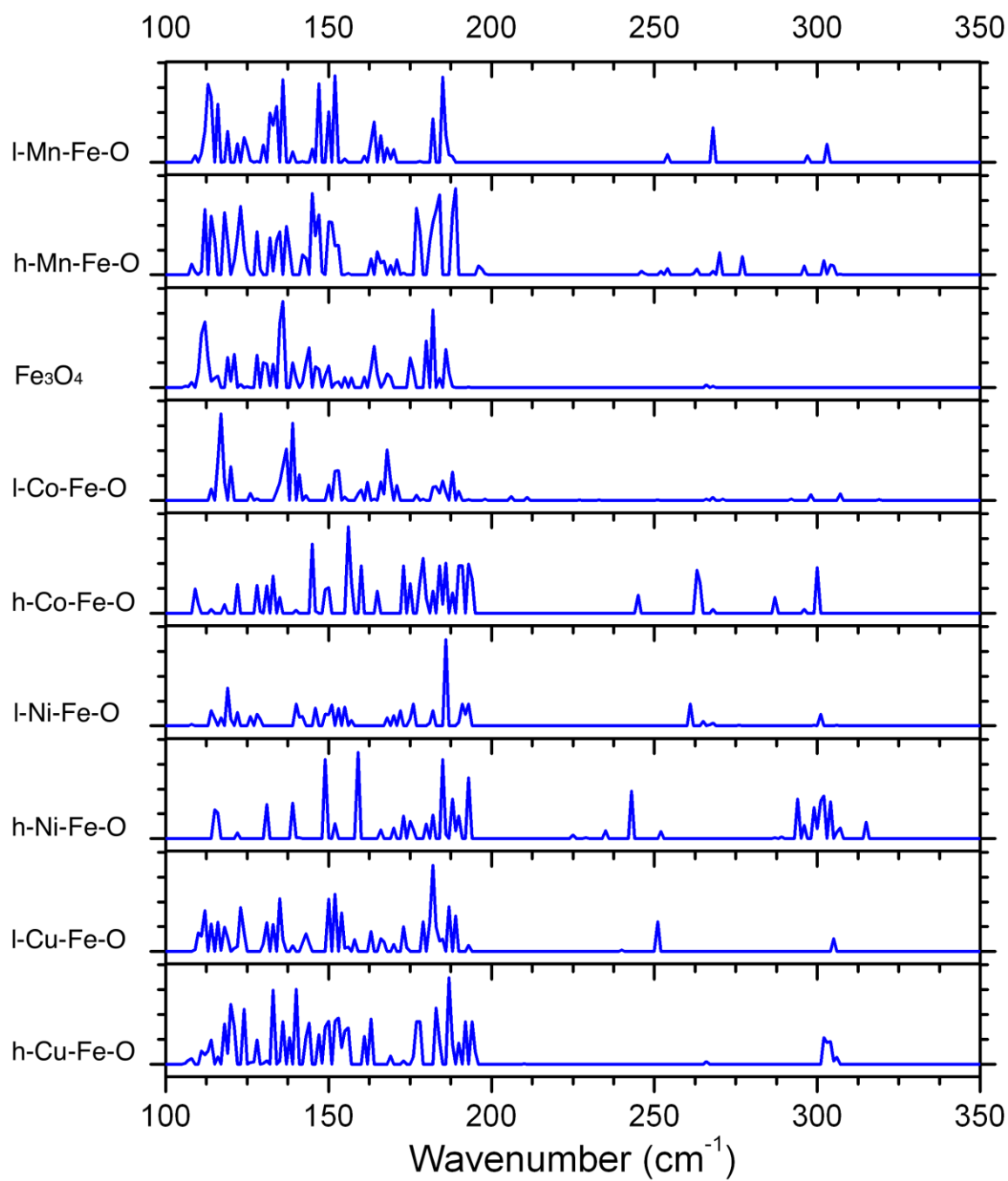


Figure S2. Collected and normalized Raman data for all growth runs acquired using the 514 nm laser line.

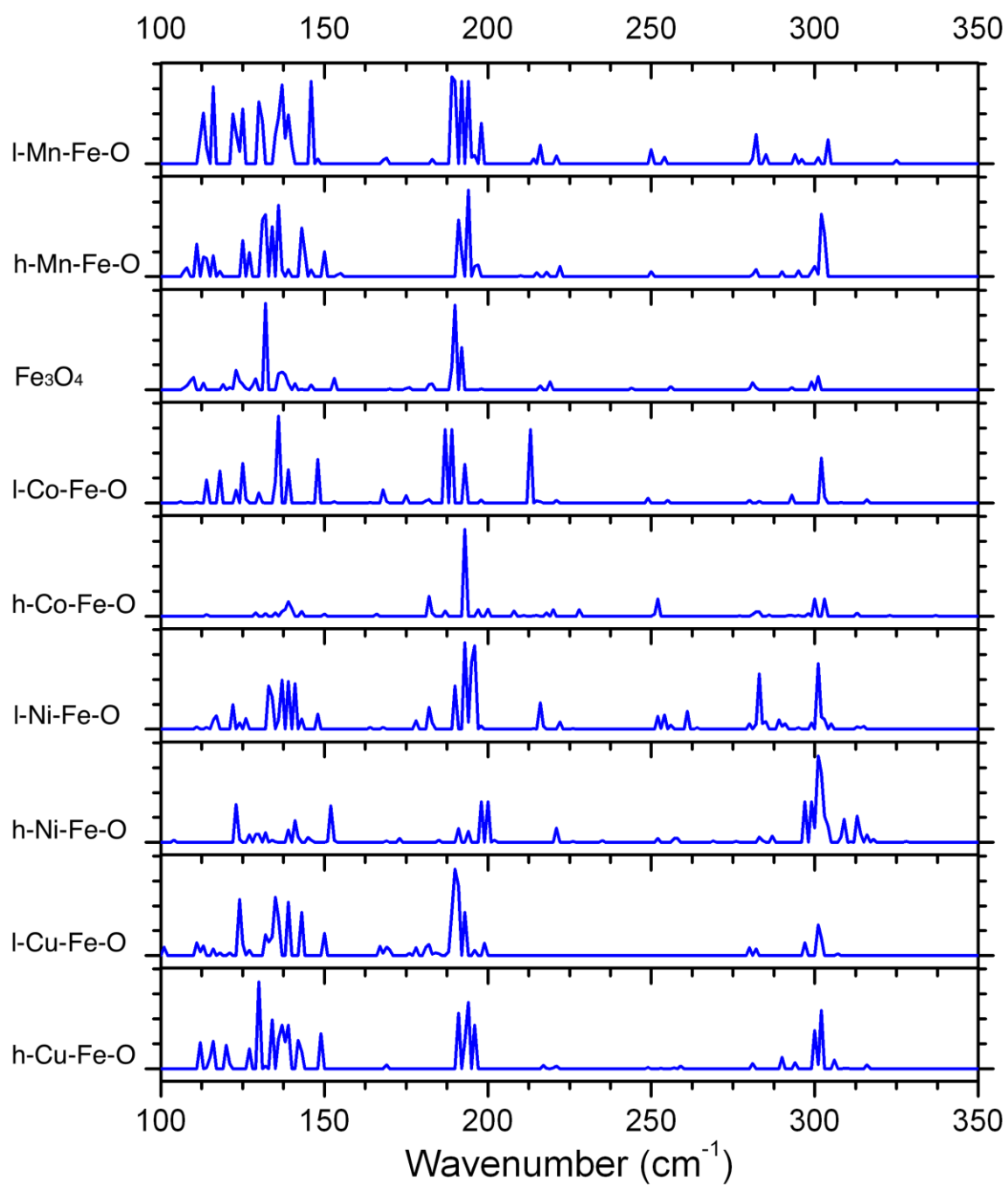


Figure S3. Collected and normalized Raman data for all growth runs acquired using the 633 nm laser line.

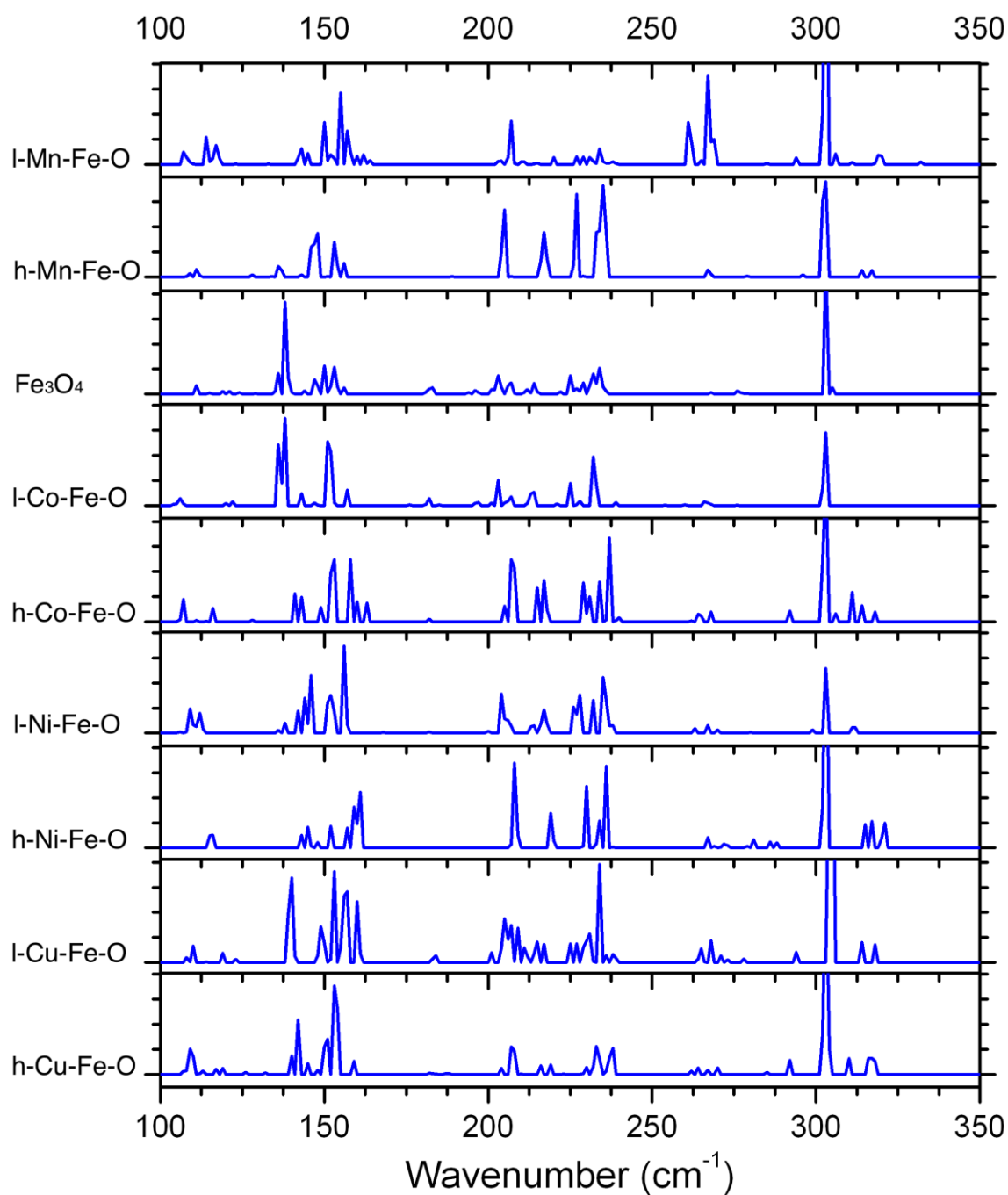


Figure S4. Collected and normalized Raman data for all growth runs acquired using the 785 nm laser line.

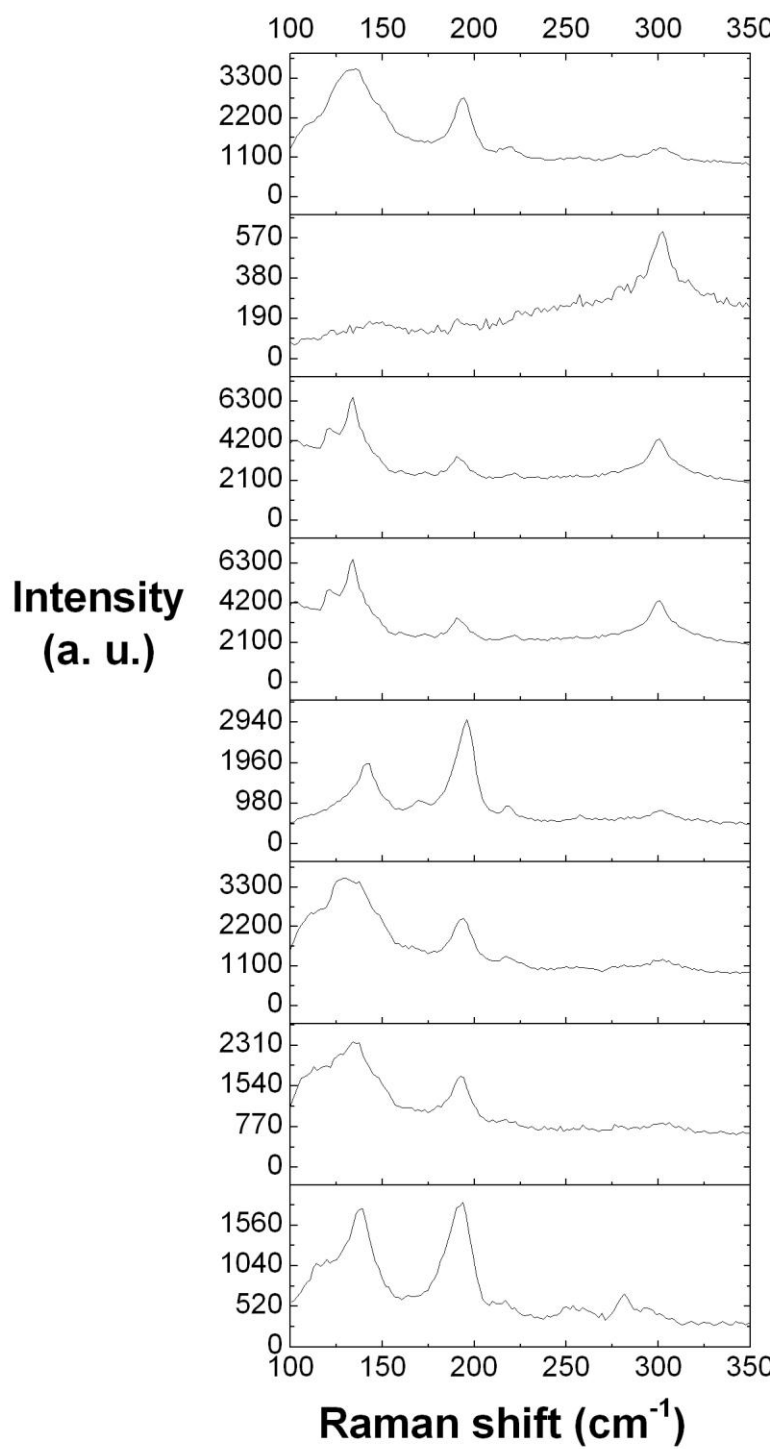


Figure S5. Collected h-Cu-Fe sample acquired using 633 nm laser wavelength.

